Canadian Conference - Pacific Conference on Earthquake Engineering 2023
Vancouver, British Columbia
June 25th – June 30th, 2023

A New Braced-Frame System For Self-Centering and Damage-Free Seismic Response For Low-Rise Steel Building Structures

Robert Tremblay[1*] and Khouzam Darwiche[2]

[1]Professor, Civil Geological and Mining Eng. Dept., Polytechnique Montréal, Montreal, QC Canada
[2]Graduate Researcher, Civil Geological and Mining Eng. Dept., Polytechnique Montréal, Montreal, QC Canada
[*]robert.tremblay@polymtl.ca (Corresponding Author)

ABSTRACT

This article describes a new concentrically braced steel frame system that can exhibit elastic bi-linear response storey shear-storey drift response in the first-storey of building structures to act as a base isolation system to achieve superior seismic performance under more frequent and smaller earthquakes as well as under design level ground motions from severe seismic events. The system comprises inverted-V braced frames (IV-BFs) with brace-to-beam connections in the first-storey that are detailed to trigger bi-linear, self-centering lateral response. V-braces acting with floor beams (VB assemblies) are also used in the first storey to develop the required first-storey shear stiffness upon activation of the IV-BFs. The nonlinear response of the system is first presented, together with the equations required to determine its stiffness property and elastic deformation capacity. The application of the system is then illustrated for 2- and 3-storey buildings located in Montreal, Quebec, and Vancouver, BC. The system is designed using the single-mode analysis method for base isolated structures that refers to effective stiffness and equivalent viscous damping properties evaluated at the target lateral displacement. Nonlinear response history analysis under unidirectional ground motion records acting independently along each building orthogonal directions is performed to evaluate the seismic response of the system. Additional NLRHA are also performed under pairs of orthogonal ground motion records with consideration of accidental eccentricity to examine the sensitivity of the system to in-plane torsional response. The results show that the proposed system can exhibit a predictable and stable self-centering bilinear elastic response without residual deformations when subjected to unidirectional ground motion records. Larger displacements were observed, however, for the buildings with accidental mass eccentricity subjected to bidirectional ground motion records.

Keywords: Inverted-V braced steel frame, self-centering nonlinear response, in-plane torsional response.

INTRODUCTION

In the last decades, there has been a growing interest in the development of new structural systems for buildings that can offer enhanced seismic performance characterized by limited storey drifts and floor accelerations and that sustain no structural damage and residual deformations, such that downtime periods and repair costs after severe earthquake events are minimized. For steel structures, controlled-rocking braced frames and braced frames with self-centering bracing members have been proposed to achieve such a superior seismic performance [1]. Base isolation also represents an effective means of protecting structures from the effects of ground motions generated by earthquake events. This strategy has been extensively studied since the early 1980's and has then been successfully implemented in practice for bridge and building structures located in active seismic regions [2-4]. Before the development of the advanced base isolation systems that are now available, the idea of minimizing the seismic demand on building structures by intentionally designing structures with a flexible first-storey had been proposed and investigated [5-6]. This option has since been investigated in several subsequent studies [7-16].

This article presents a study that was performed to examine the potential of using an inverted-V steel braced frame system specially designed and detailed to display under moderate and severe seismic events a stable bilinear elastic response in the first storey of low-rise steel buildings in case of moderate and severe seismic events to create a base isolated structure. In this braced frame system, nonlinear response is obtained from brace-to-beam end plate connections that transmit compression loads through direct bearing. Upon tension, a gap opens in the connections, which significantly reduces the braced frame

lateral stiffness. The brace-to-beam connections also include bolted lap splices designed to slip and dissipate energy through friction upon gap opening and closing. The bracing members and the beam intersected by the braces are sized to resist forces expected at the target first storey drift to develop elastic self-centering response. Additional V-brace/beam assemblies can be introduced are introduced in the building first-storey to achieve sufficient lateral stiffness upon activation of the inverted-V braced frames.

Preliminary design of the system can be performed using the simplified single-mode method widely adopted for the design of base isolation systems. In that method, the isolated structure system is represented by a single-degree-of-freedom system with effective period and equivalent viscous damping properties. The structure response can then be verified through nonlinear response history analyses and the system properties adjusted as needed to meet project specific objectives in terms of peak lateral displacements, floor accelerations and/or lateral loads. In Canada, although now extensively used for bridge structures, the base isolation solution has not been frequently adopted for building structures, mainly because of the cost of the isolation units and the additional foundation work required to house the isolation system and accommodate the large displacements expected at the building base. In this context, the braced frame system examined in this study could represent a simple and cost-effective alternative means of obtaining base isolated structures, together with the advantages in terms of enhanced seismic response and resiliency. A description of the proposed system given in the first section of the article, together with the equations that can be used to determine the properties of the system that govern its elastic nonlinear response. The design of the system is then illustrated for 2- and 3-storey buildings located in Montreal, QC, and Vancouver, BC. The seismic response of the structures is thereafter examined using nonlinear response history analyses under site representative ground motions. The analyses are first performed independently in each orthogonal direction of the buildings. They are subsequently repeated using pairs of orthogonal ground motion records and considering accidental mass eccentricity to examine the sensitivity of the proposed system to in-plane torsional response.

PROPOSED SYSTEM

Description

The proposed system includes two main structural components: inverted V-braced frames (IV-BFs) that are designed to resist lateral wind loads in the elastic range and develop a bilinear self-centering storey response under moderate and severe seismic events, and V-braces/beam (VB) assemblies that are used to provide additional elastic stiffness upon nonlinear IV-BF seismic response. The two components are illustrated in Figure 1, and a detail of the brace-to-beam connections of the IV-BFs is presented in Figure 2. In these connections, end plates welded to the braces and gusset plates are used to transmit compression loads through by means of direct bearing. Bolted connections designed to slip at a load F_s are also provided to transmit brace tension loads. The slip resistance F_s acts in combination with the brace compression loads from gravity loads on the beam to resist wind induced lateral loads. Under a severe earthquake, tension loads in the braces will reach the slip load F_s, which will trigger opening of a gap in the tension brace connection. The first-storey lateral stiffness will then reduce to that obtained from the compression brace acting in series with the beam deforming in flexure. Pairs of V-braces placed on either side of gravity columns in the first storey act in combination with the floor beams to which they are connected can be used as necessary in the building to achieve the target first-storey stiffness upon nonlinear response of the IV-BFs.

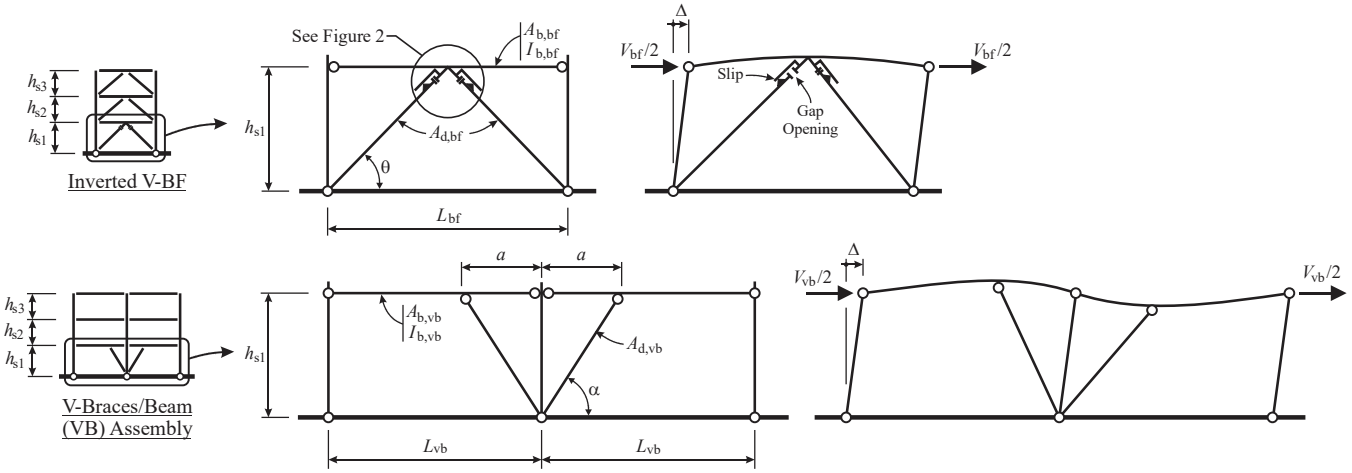

Figure 1. Geometry of the inverted-V braced frame (IV-BF) and V-braces/beam (VB/Beam) assembly.

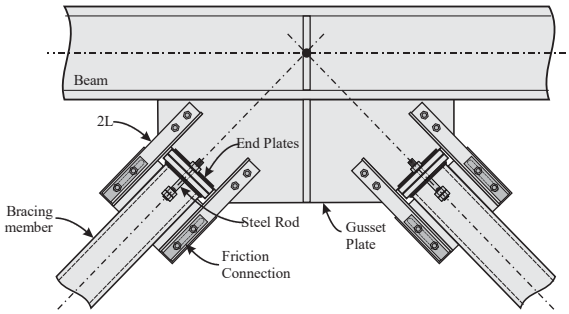

Figure 2. Brace-to-beam connections in IV-BFs.

Response of the system

The lateral stiffness of the first level of an IV-BF prior to and after initiation of slippage in the brace connections, $K_{bf,1}$ and $K_{bf,2}$, respectively, can be obtained from:

$$\frac{1}{K_{bf,1}} = \frac{L_{bf}}{4EA_{b,bf}} + \frac{L_{bf}}{4EA_{d,bf}\cos^3\theta} \tag{1}$$

$$\frac{1}{K_{bf,2}} = \frac{L_{bf}}{4EA_{b,bf}} + \frac{L_{bf}}{2EA_{d,bf}\cos^3\theta} + \frac{L_{bf}^3\tan^2\theta}{48EI_{b,bf}} \tag{2}$$

, whereas the lateral stiffness contributed by an VB/Beam assembly, K_{vb}, can be determined from:

$$\frac{1}{K_{vb}} = \frac{a}{2EA_{d,vb}\cos^3\alpha} + \frac{a^2\left(L_{vb}-a\right)^2\tan^2\alpha}{6EI_{b,vb}L_{vb}} \tag{3}$$

In low-rise steel buildings, columns are typically continuous over the full building height. Those columns will be subjected to bending when the building lateral deformations will concentrate in the first-storey initiation of nonlinear response in the IV-BFs. The resistance of the building columns to that bending demand will contribute an additional lateral stiffness K_c to the first storey. That stiffness can be estimated using the expressions in Eq. (4a) for 2-storey buildings, K_{c2}, and Eq. (4b) for 3-storey buildings, K_{c3}. Those simple expressions have been derived assuming the columns are pin connected at their bases and that the storey drifts in the second and third levels are small and can be neglected.

$$K_{c,2} \approx \frac{3\sum\left(EI_c\right)}{h_{s1}^3 + h_{s1}^2 h_{s2}} \tag{4a}$$

$$K_{c,3} \approx \frac{3\sum\left(EI_c\right)}{h_{s1}^3 + 0.875\,h_{s1}^2 h_{s2}} \tag{4b}$$

Slippage in the IV-BF tension brace connection will occur under a lateral load $V_{bf,s}$ that can be calculated with Eq. (5a) for beams supporting a uniformly distributed gravity load w and with Eq. (5b) for beams supporting two equally spaced gravity point loads P:

$$V_{bf,s} = 2F_s\cos\theta + \frac{0.625\,w\,L_{bf}}{\tan\theta} \tag{5a}$$

$$V_{bf,s} = 2F_s\cos\theta + \frac{15P}{4\tan\alpha} \tag{5b}$$

, and the first-storey drift at initiation of brace connection slip is $\Delta_{bf,s} = V_{bf,s} / K_{bf,1}$. The resulting hysteretic response of an IV-BF is illustrated in Figure 3a. As shown, this is partial self-centering response with self-centering capacity depending on the values of $V_{bf,s}$ and F_s. Under gradually incremented lateral loads, yielding will eventually develop in the IV-BF and VB beams due to combined axial and bending moments. In this study, the storey shear at level 1 required to form a plastic hinge in the beam of those beams, $V_{bf,y}$ and $V_{bb,y}$ respectively, can be determined from static analysis using the cross-sectional strength interaction equation of CSA S16-19 [19] for Class 1 and Class sections of I-shaped members under axial

compression and bending and the probable beam axial and flexural resistances calculated with the beam probable yield stress R_yF_y. For the VB-assemblies, the corresponding first-storey drift is $\Delta_{vb,y} = V_{vb,y} / K_{vb}$. For the IV-BFs, $\Delta_{bf,y}$ is obtained from:

$$\Delta_{bf,y} = \Delta_{bf,s} + \left(V_{bf,y} - V_{bf,s}\right)\Big/ K_{bf,2} \tag{6}$$

The resulting storey shear-storey drift response of the building first-storey is illustrated in Figure 3b. As shown, the response includes contributions from all IV-BFs and VB assemblies acting along the building direction considered, ΣK_{bf} and $\Sigma K_{vb,}$ as well as that from all columns in the buildings, ΣK_c. In design, beam sections for the IV-BFs and VB assemblies are selected such that $\Delta_{bf,y}$ and $\Delta_{vb,y}$ exceed by a sufficient margin the target first-storey drift Δ_t to ensure elastic self-centering response. The columns are also designed as beam-column elements to resist the axial compression from concomitant gravity loads combined with the bending moment induced by the first-storey drift.

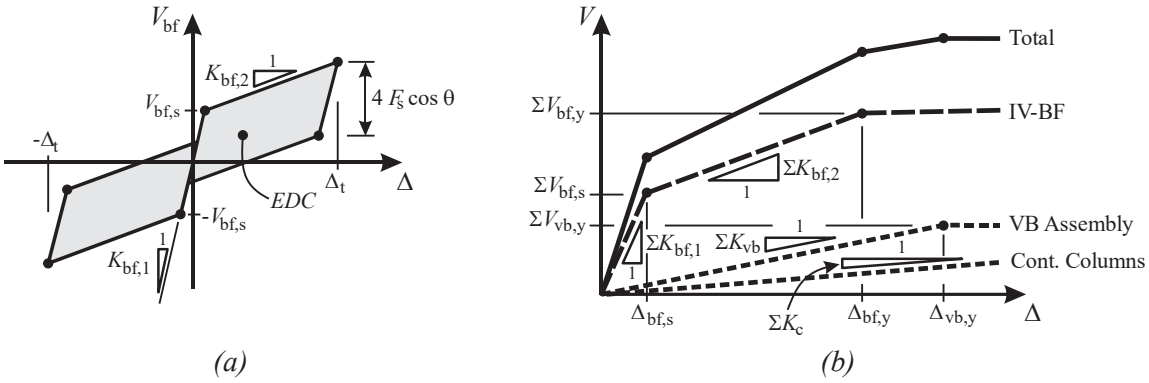

Figure 3. (a) Hysteretic response of the IV-BFs; (b) First storey shear-storey drift response of the system the system.

As indicated, the single-mode approach used for base isolation systems can be adopted to determine the properties of the system that are required to limit the first-storey drift to the target value, Δ_t. This approach is based on the effective period, T_{eff}, and equivalent viscous damping ratio, ξ, of the system at the target first-storey drift. The period T_{eff} is determined assuming that the building lateral response is dominated by the first-storey effective stiffness at the target storey drift, K_{eff}, and the total building seismic weight, W. For a structure designed with n_{bf} identical IV-BFs and n_{vb} identical VB assemblies, T_{eff} is then given by:

$$T_{eff} = 2\pi\sqrt{\frac{W}{g\,K_{eff}}}\ \text{, where: } K_{eff} = n_{bf}\,\frac{V_{bf,s} + K_{bf,2}\left(\Delta_t - \Delta_{bf,s}\right)}{\Delta_t} + n_{vb}\,K_{vb} + \sum K_c - \frac{\sum C_f}{h_{s1}} \tag{7}$$

In the expression for K_{eff}, the last term represents the negative stiffness induced by P-delta effects due to the axial compression loads from concomitant gravity loads C_f carried by all columns in the first-storey, as these effects can be significant on the response of structures with a soft first storey [16]. The equivalent damping at the target storey drift Δ_t is a function of the energy per cycle of amplitude Δ_t dissipated by each of the n_{bf} IV-BFs, EDC_{bf}:

$$\xi = \frac{1}{2\pi}\frac{n_{bf}\,EDC_{bf}}{K_{eff}\,\Delta_t^2}\ \text{, where: } EDC_{bf} = 2\left(4F_s\cos\theta\right)\Delta_t = 8F_s\cos\theta\,\Delta_t \tag{8}$$

As will be discussed in the next section, the values of T_{eff} and ξ to limit the storey drift to Δ_t can be determined from site-specific nonlinear displacement spectra derived for single-degree-of-freedom self-centering systems exhibiting different properties.

SEISMIC DESIGN AND RESPONSE OF THE PROPOSED SYSTEM FOR 2- AND 3-STOREY BUILDINGS

To verify the systems seismic response and validate the proposed design procedure, the system was used for 2- and 3-storey office building structures located in Montreal, QC, for eastern Canada and Vancouver, BC, for western Canada. The geometry of the buildings studied is described in Figure 4, together with elevation views of the IV-BFs and VB assemblies used in each of the building orthogonal directions. Note that the structure plan view shown is for the floor levels. The floor dead load is 4.58 kpa and the weight of the exterior wall is 1.5 kPa. The occupancy floor live loads are indicated in the figure. A lighter structural system comprising a 38 mm deep steel deck panels placed on open web steel joists seating on roof girders is used for the roof. The roof dead load is 1.2 kPa and design roof snow loads equal to 2.48 and 1.64 kPa were used for the Montreal and Vancouver sites, respectively.

For Montreal, a soft site with an average shear wave velocity $V_{s,30}$ = 300 m/s was selected as this condition was expected to result in larger lateral displacement demand. Similarly, for Vancouver, a site with $V_{s,30}$ = 360 m/s was chosen. The site-specific NBC 2020 seismic hazard values used for the design and analysis of the buildings were obtained from the NBC 2020 Seismic Hazard Tool [19]. Those are plotted in Figure 8. According to NBC 2020, the Montreal and Vancouver sites are designated as Site Category 3 (SC3) and Site Category 4 (SC4), respectively. Site categories are used later in the building ID. For example, building SC3-3 is the 3-storey building in Montreal.

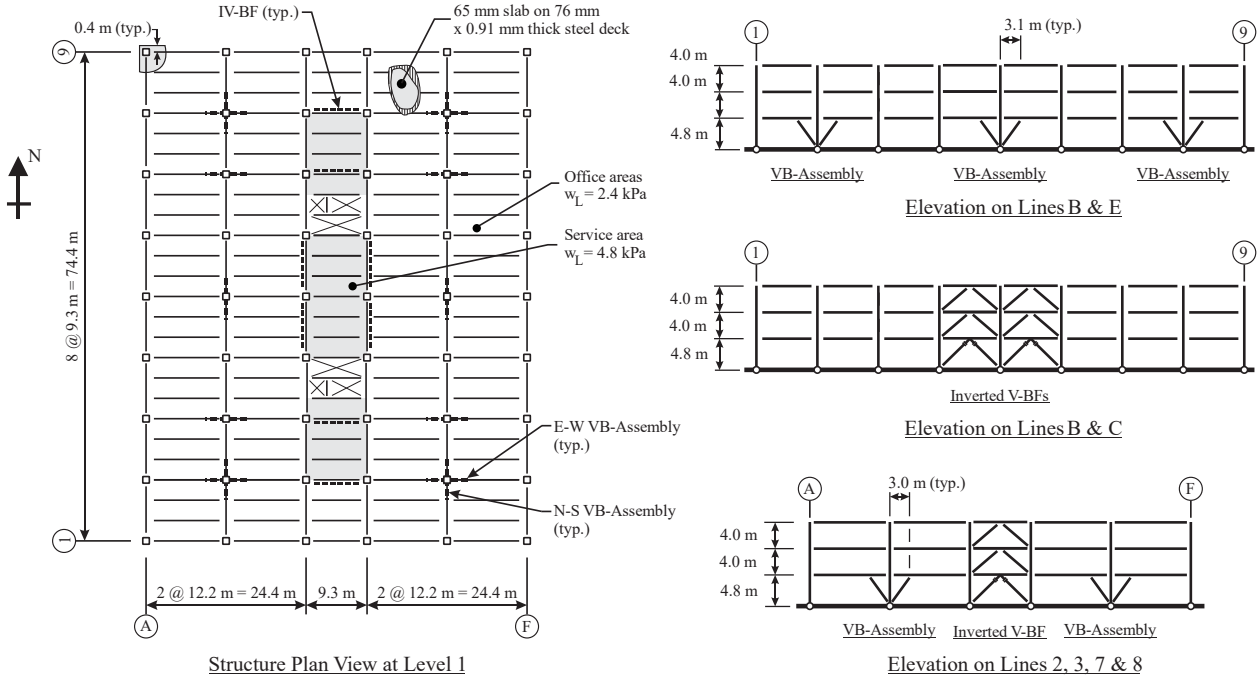

Figure 4. Geometry of the building structures studied.

For the selection of suitable effective period T_{eff} and equivalent damping properties, nonlinear response analyses were conducted on single-degree-of-freedom systems exhibiting a self-centering response as illustrated in Figure 5. A total of 875 systems were studied by varying the following properties: initial elastic period T_e = 0.4, 0.5, 0.6, 0.7, and 0.8 s, by modifying the initial stiffness k_1; the base shear $V_1 = S \cdot W/R$ where S is the NBC 2020 design spectrum at the site and R = 6, 7, 8, 9, and 10; the stiffness ratio k_2/k_1 = 0.08, 0.10, 0.12, 0.14, and 0.16; and the amount of energy dissipation with β = 0.5, 0.6, 0.7, 0.8, 0.9, 1.0, and 1.1. For each site, the systems were subjected to ensembles of site representative ground motion records: 32 records for Montreal and 40 records for Vancouver.

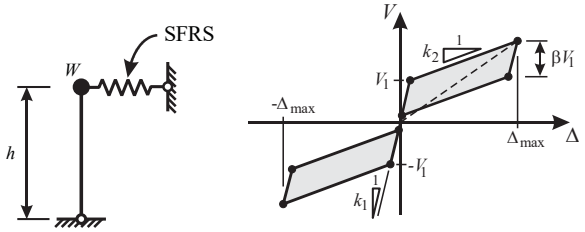

Figure 5. Single-Degree-of-Freedom system with self-centering hysteretic response.

The analyses were performed with the OpenSees program [17] using the SelfCentering material and 3% mass proportional damping, which is representative for steel structures. For each record, the effective stiffness K_{eff}, the effective period T_{eff}, the energy dissipation EDC, and the equivalent damping ratio ξ_{eq} were determined at the peak displacement Δ_{max} reached in the analysis, and the mean peak displacement values for all ground motion records are plotted as a function of the mean period T_{eff} in Figure 6. In the figure, the displacement results are also grouped as a function of the equivalent damping ranges, ξ_{eq} = 0-5%, 5-10%, 10-15%, 15-20%, and 20-25%.

As shown in Figure 3, the structure is symmetrical in plan, with four IV-BFs and four VB assemblies acting in each direction. The design was therefore performed independently along each orthogonal direction of the building. Accidental in-plane

eccentricity was ignored and the total lateral load demand was assumed to be equally distributed among the IV-BFs and VB assemblies. For the structures in Montreal, a target first-storey drift of 1% h_{s1} (Δ_1 = 48 mm) was adopted for design, which corresponds to the NBC limit for post-disaster buildings. From Figure 6a, it is seen that this can be achieved with T_{eff} of approximately 1.0 s and equivalent viscous damping of 5-10%. Larger displacement demand is expected in Vancouver, and a target drift of 1.3% h_{s1} (Δ_1 = 62 mm) was selected. Results in Figure 6b show that this value can be obtained with $T_{eff} \approx$ 0.8-0.9 s and approximately 10% equivalent damping. Using the equations presented in the previous section, the slip load F_s and member sections were selected to obtain those properties. The bracing members are square ASTM A1085 HSS profiles and the beams are ASTM A992 W shapes. The selected slip loads F_s and sections are given in Table 1. The resulting stiffness properties of the IV-BFs and VB assemblies are presented in Table 2, together with the effective period and equivalent damping properties for the whole buildings. The base shear *vs* storey drift monotonic responses predicted along both directions of all buildings are presented in Figure 7. To account for the variability in ground motions and their effects, beam sections were chosen so that plastic hinging would form at a storey drift larger than the target ones. At both sites, a margin of approximately 1.5 could be achieved in the E-W direction. In the N-S direction, however, the margins between drifts at beam yielding and target drifts are smaller because the girders have shorter spans and carry higher gravity loads.

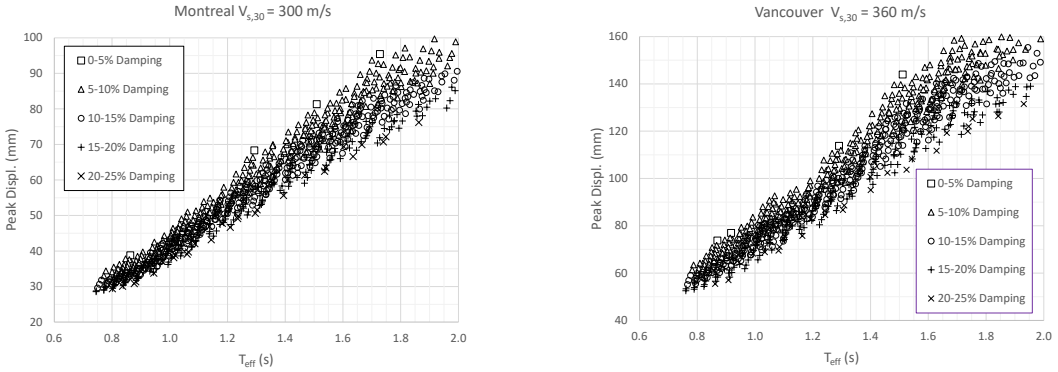

(a) *(b)*

Figure 6 Expected man peak lateral displacements of self-centering systems in: (a) Montreal; and (b) Vancouver.

Table 1. Selected shapes for beams and bracing members of IV-BFs and VB-Assemblies.

No.	Dir.	Level	IV-BFs			VB Assemblies	
			Bracing members	Beams	F_s (kN)	Bracing members	Beams
SC3-2	E-W	2	HSS 152x152x7.9	-	-	-	-
		1	HSS 203x203x9.5	W360x287	200	HSS 152x152x9.5	W610x125
	N-S	2	HSS 152x152x7.9	-	-	-	-
		1	HSS 203x203x12.7	W360x421	200	HSS 152x152x9.5	W610x155
SC3-3	E-W	3	HSS 152x152x7.9	-	-	-	-
		2	HSS 152x152x9.5	-	-	-	-
		1	HSS 203x203x15.9	W360x347	250	HSS 178x178x9.5	W610x155
	N-S	3	HSS 152x152x7.9	-	-	-	-
		2	HSS 152x152x9.5	-	-	-	-
		1	HSS 203x203x15.9	W360x463	250	HSS 178x178x9.5	W610x155
SC4-2	E-W	2	HSS 152x152x9.5	-	-	-	-
		1	HSS 203x203x15.9	W360x347	350	HSS 203x203x9.5	W610x155
	N-S	2	HSS 152x152x7.9	-	-	-	-
		1	HSS 203x203x15.9	W360x463	350	HSS 178x178x9.5	W610x174
SC4-3	E-W	3	HSS 152x152x7.9	-	-	-	-
		2	HSS 152x152x9.5	-	-	-	-
		1	HSS 203x203x15.9	W360x421	500	HSS 203x203x9.5	W610x174
	N-S	3	HSS 152x152x7.9	-	-	-	-
		2	HSS 152x152x9.5	-	-	-	-
		1	HSS 203x203x15.9	W360x551	500	HSS 203x203x9.5	W610x174

Table 2. Stiffness properties of the proposed system as designed

No.	Dir.	$K_{bf,1}$ (kN/mm)	$K_{bf,2}$ (kN/mm)	K_{vb} (kN/mm)	ΣK_c (kN/mm)	$\Sigma C_f/h_{s1}$ (kN/mm)	K_{eff} (kN/mm)	W (kN)	T_{eff} (s)	ξ (%)
SC3-2	E-W	195	10.1	6.48	5.18	7.6	173	29280	0.83	8.5
	N-S	254	15.8	12.5			217		0.74	6.8
SC3-3	E-W	300	12.9	8.36	10.3	10.9	138	48960	1.19	13.3
	N-S	306	17.9	13.0			236		0.91	7.8
SC4-2	E-W	300	13.0	8.52	6.44	7.4	224	28350	0.71	8.9
	N-S	306	17.9	14.4			232		0.70	8.6
SC4-3	E-W	304	16.1	9.55	15.0	10.7	176	48030	1.05	16.2
	N-S	309	21.8	14.8			267		0.85	10.6

Notes: $K_{bbf,1}$, $K_{bf,2}$, and K_{vb} are per frame; ΣK_c, $\Sigma C_f/h_{s1}$, K_{eff}, W, T_{eff}, and ξ are for the entire building.

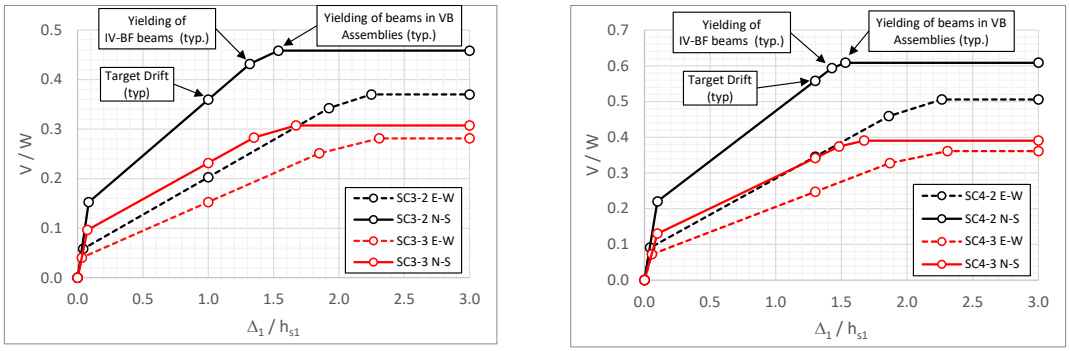

(a) *(b)*

Figure 7. Base shear vs storey drift in Level 1 for the structures in: (a) Montreal; and (b) Vancouver.

Columns were designed with factored resistances sufficient to carry the factored axial compression from concomitant gravity loads D+0.5L+0.25s combined with bending moments induced by first-storey drifts equal to 1.5 times the target storey drifts. Square HSS profiles were used for the columns as this section has equal flexural resistance in both directions and is not prone to lateral-torsional buckling.

Nonlinear response history analysis (NLRHA) of the structures was performed with the SAP2000 computer program [21] using three-dimensional models as shown in Figure 8 for the 2-storey buildings. Nonlinear link elements were used to simulate the brace-to-beam connection response in the IV-BFs, with gap elements for direct contact in compression and Wen for the friction upon gap opening and closing. Plastic hinges with P-M_3 interaction were assigned to the beams of the IV-BFs and VB assemblies, whereas plastic hinges with P-M_2-M_3 interaction were assigned at the top end of the first-storey columns. Rigid diaphragm was assigned at each level. In the NLRHA, P-delta effects were considered in the NLRHA with gravity loads due to D+0.5L+0.25 S.

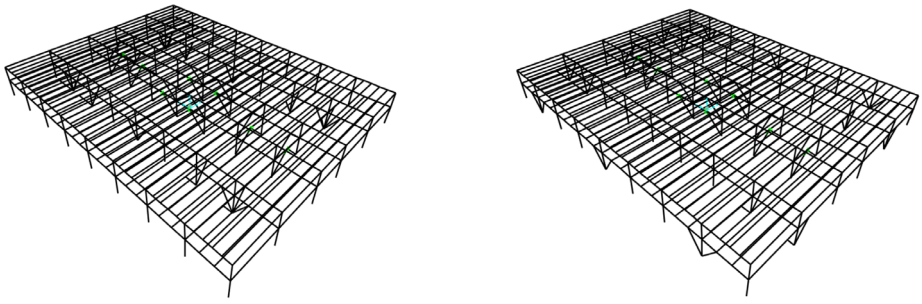

(a) *(b)*

Figure 8. SAP2000 models of the 2-storey structures studied: (a) Original configuration with VB positioned along interior column lines; (b) Modified configuration with VB assemblies repositioned along the exterior column lines.

Rayleigh damping corresponding to 3% in first and second translational modes of vibrations. Stiffness proportional damping was assigned to the material of the frame members to avoid the development of spurious damping forces in the nonlinear link

elements. Two series of NLRHA were conducted. In the first one, ground motion (GM) records were applied independently in the E-W and N-S directions. In the analyses, lateral displacements in the direction perpendicular to the applied ground motions were blocked in the model. This first NLRHA series aimed at investigating the unidirectional response of the system to verify its behaviour and validate the applicability of the base isolation single-mode method for predicting lateral displacements of the system. In the second NLRHA series, pairs of orthogonal GM records were applied simultaneously to the structure. In that case, the model was free to sustain lateral displacements along both orthogonal directions as well as in-plane rotation. In the model, accidental eccentricity was considered by displacing the center of mass towards both the East and North directions by 5% of the E-W and N-S building dimensions, respectively.

The computed periods of the structures are presented in Table 3. For the study of the system response under unidirectional ground motion records, the models with the translational displacements blocked in the direction perpendicular to the direction of the ground motion record were used in the modal analyses and T_1 and T_2 then correspond to the first and second translational mode periods in the direction of NRLHA. In the models used for bidirectional response, periods T_1 and T_4 are those associated with the first and second torsional modes of vibrations, periods T_2 and T_5 are those associated with the first and second E-W translational modes, whereas periods T_3 and T_6 are those of the first and second N-S translational modes. As shown, all structures are slightly stiffer in the N-S directions as the periods related to N-S translation are shorter than the corresponding ones in the E-W direction. It is noted that all structures are flexible in torsion as their periods associated to the first two torsional modes are longer than those of the two translational modes.

Table 3. Computed periods of the structures studied.

No.	***Unidirectional Response***			***Bidirectional Response*[1]**					
	Dir.	T_1 **(s)**	T_2 **(s)**	T_1 **(s)**	T_2 **(s)**	T_3 **(s)**	T_4 **(s)**	T_5 **(s)**	T_6 **(s)**
SC3-2	E-W	0.46	0.20	0.55 (T)	0.45 (E-W)	0.41 (N-S)	0.25 (T)	0.20 (E-W)	0.19 (N-S)
	N-S	0.42	0.19						
SC3-3	E-W	0.57	0.24	0.70 (T)	0.56 (E-W)	0.53 (N-S)	0.29 (T)	0.23 (E-W)	0.21 (N-S)
	N-S	0.54	0.22						
SC4-2	E-W	0.33	0.17	0.40 (T)	0.33 (E-W)	0.31 (N-S)	0.20 (T)	0.17 (E-W)	0.15 (N-S)
	N-S	0.32	0.15						
SC4-3	E-W	0.51	0.20	0.62 (T)	0.50 (E-W)	0.48 (N-S)	0.25 (T)	0.20 (E-W)	0.19 (N-S)
	N-S	0.49	0.19						

[1]Note: (E-W) & (N-S) = Translational modes in E-W and N-S directions; (T) = Torsional modes

For both series of NLRHA, ensembles of site-representative ground motion records were selected and scaled in accordance with the guidelines of Commentary I of NBC 2020. For the first NLRHA series, the ensembles included single-component GM records. For the Montreal site, 3 records from small magnitude EQs at shorter distances (M5.91-6.19 at 7.6-28.6 km) and 8 records from larger magnitude earthquakes at longer distances (M6.5-7.01 at 8.5-54.8 km). For Vancouver, the ensemble included 6 records from crustal (CR) EQs, 5 records from in-slab (IS) EQs, and 11 records from interface subduction (IF) EQs. For the second NLRHA series, pairs of orthogonal GM record components were used and scaled using the geomean spectrum of the individual components. For Montreal, the ensemble comprised 4 records from small EQs at short distances (M5.25-6.91 at 7.6-27.6 km) and 7 records from larger magnitude EQs at longer distances (M6.53-7.51 at 11.1-54.8 km). The ensemble for Vancouver included records from 6 CR EQs, 5 IS EQs, and 11 IF EQs. Because the selection of ground motion records was essentially based on the match between the spectra of the GM records and the UHS, and geomean spectra of component spectra were used for the second NLRHA series, the ensembles used in the two series of analyses do not contain the same GM records. The 5% damped acceleration spectra of the selected and scaled records are plotted in Figure 8.

A typical response obtained from the first NLRHA series is presented in Figure 9 for the SC4-3 building subjected to a crustal EQ GM applied along the E-W direction. As intended, storey drifts concentrated in the first storey with a peak value of 1.5% h_{s1} and storey drifts in the 2nd and 3rd levels limited to 0.3% h_{s2} and 0.15% h_{s3}, respectively. The system exhibited a stable bi-linear elastic response and, thereby, did not sustain any residual deformations at the end of the ground motion. The history of the vertical displacement of the beam at mid-span of the E-W IV-BF is also shown in Figure 9a. The beam upward deformation reached 60 mm during the EQ, which corresponds to 1/155 of the beam span. The beam remained elastic and could return to its original position at the end of the EQ. Beams of the VB assemblies and columns also remained elastic.

Mean values and ranges of the peak storey drifts in the first level from the first NLRHA series (unidirectional response) are presented in Table 4. For the two buildings in Montreal, the mean values range from 0.85 to 1.07% h_{s1}, which is close to the design target value of 1.0% h_{s1}. For the two buildings in Vancouver, the mean drift values vary from 0.96 to 1.37% h_{s1}, which also agrees well with the 1.3% h_{s1} target value adopted in design. For all buildings, peak storey drifts are smaller along the N-S direction, which can be attributed to the system shorter effective periods along that direction. For the buildings studied and

GM records considered, the ratios between maximum and mean storey drifts for a given GM ensemble vary between 1.32 and 1.64, suggesting that keeping a margin of 1.5 between the storey drifts that trigger beam yielding in the IV-BFs and VB assemblies and the target storey drift could represent a reasonable design approach. For the buildings in Vancouver, mean drift values in table 4 are for the entire suite of 22 GM records. Examination of the results show that mean peak drifts from the 11 interface subduction (IF) GM records are between 0.71 and 0.88 times the man drift values from the suite of crustal and in-slab ground motions, which indicates that the proposed system with elastic self-centering response can be effective in limiting lateral displacements under long duration EQ ground motions. Values of peak horizontal accelerations at all building levels are presented in Table 5. As shown, peak floor accelerations for unidirectional responses vary from 0.11 to 0.27 g and from 0.21 to 0.57 g for the buildings in Montreal and Vancouver, respectively. Slightly higher values varying between 0.13 and 0.60 g developed at the roof level of the buildings, which was expected as the structure response remained linear elastic above the first level and the response at the roof level was affected by the building higher vibration modes. The observed accelerations are generally lower than the 2% in 50 years peak ground accelerations of 0.482 and 0.476 g for the Montreal and Vancouver sites, respectively, confirming that the proposed system can offer the same benefits as base isolation systems.

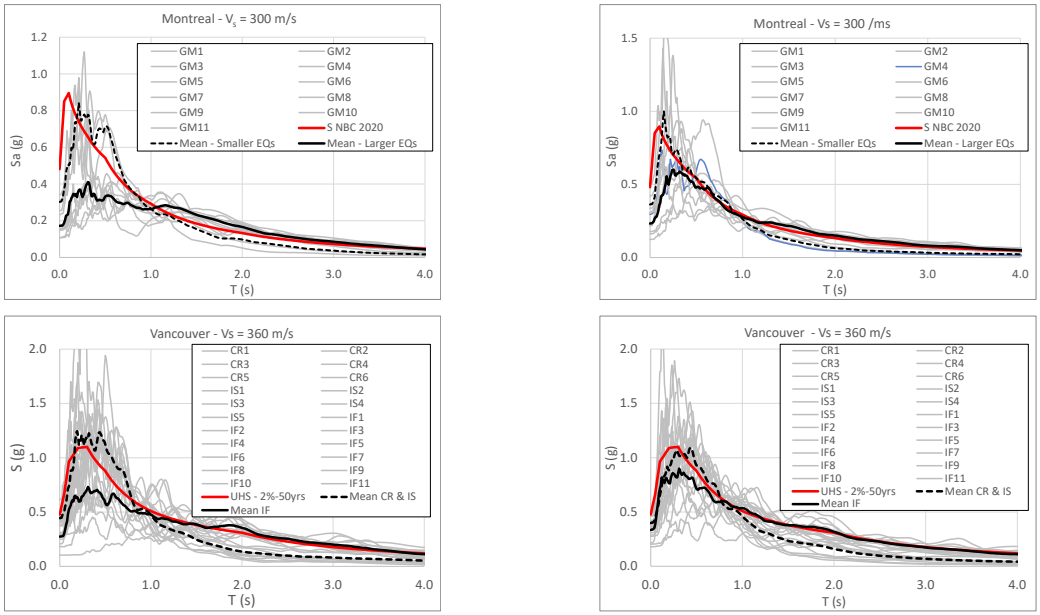

(a) *(b)*

Figure 8. 5% Damped acceleration spectra of the selected and scaled GM records: (a) Unidirectional GM records; (b) Geomean spectra of orthogonal GM record pairs.

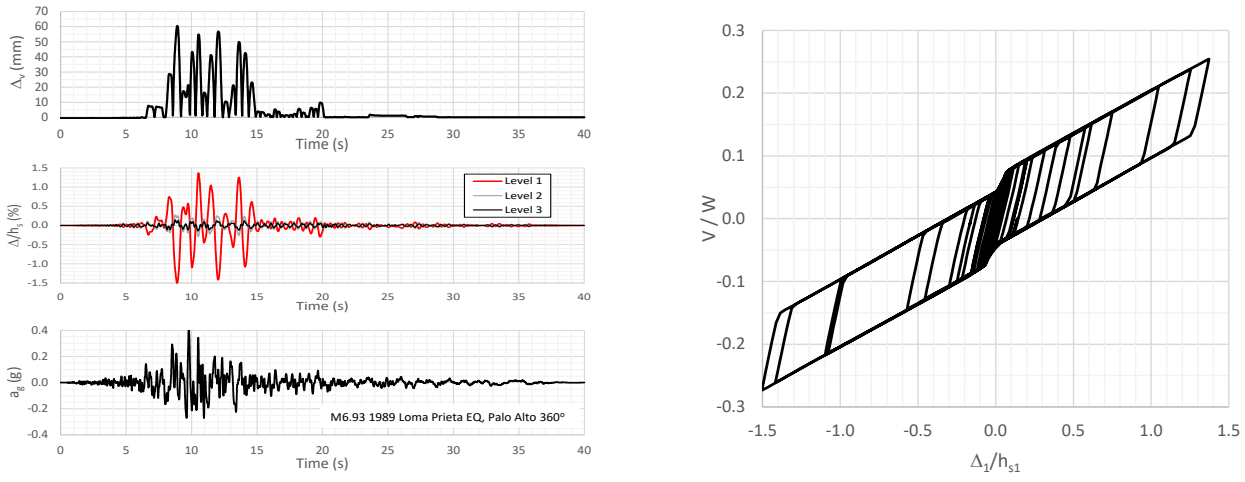

(a) *(b)*

Figure 9. E-W response of the SC4-3 structure under a crustal EQ GM record: (a) Mid-span vertical deflection of the IV-BF beam (top), storey drifts at levels 1, 2 and 3 (middle), and GM record (bottom); (b) Base shear vs storey drift at level 1.

Table 4. Peak storey drift in first level, Δ/h_{s1} (%)

No.	Dir.	*Unidirectional Response*		*Bidirectional Response at*			
				IV-BFs		*Corners*	
		Mean	*Range*	*Mean*	*Range*	*Mean*	*Range*
SC3-2	E-W	1.07	0.76 - 1.44	1.18	0.41 – 2.32	1.23	0.41 – 2.45
	N-S	0.88	0.64 - 1.21	1.01	0.60 – 1.88	1.12	0.65 – 1.91
SC3-3	E-W	1.16	0.80 - 1.57	1.25	0.46 – 2.51	1.33	0.54 – 2.66
	N-S	0.85	0.35 - 1.12	1.08	0.64 – 1.81	1.22	0.76 – 2.03
SC4-2	E-W	1.08	0.10 – 1.71	1.33	0.30 – 2.58	1.42	0.34 – 2.74
	N-S	0.96	0.05 – 1.58	0.83	0.18 – 1.58	0.97	0.23 – 1.67
SC4-3	E-W	1.37	0.40 – 1.99	1.65	0.57 – 3.05	1.74	0.64 – 3.21
	N-S	1.24	0.27 – 1.88	1.23	0.45 – 1.91	1.42	0.46 – 2.17

Table 5. Peak horizontal acceleration (g)

No.	Dir.	*Level*	*Unidirectional Response*		*Bidirectional Response*	
			Mean	*Range*	*Mean*	*Range*
SC3-2	E-W	2	0.17	0.13 – 0.20	0.22	0.15 – 0.32
		1	0.15	0.11 – 0.18	0.18	0.13 – 0.28
	N-S	2	0.19	0.14 – 0.24	0.24	0.16 – 0.35
		1	0.17	0.12 – 0.22	0.21	0.15 – 0.32
SC3-3	E-W	3	0.24	0.19 – 0.28	0.34	0.24 – 0.50
		2	0.18	0.14 – 0.23	0.23	0.15 – 0.37
		1	0.19	0.15 – 0.23	0.23	0.15 – 0.32
	N-S	3	0.28	0.17 – 0.33	0.39	0.28 – 0.48
		2	0.19	0.12 – 0.23	0.26	0.19 – 0.36
		1	0.21	0.14 – 0.27	0.27	0.20 – 0.36
SC4-2	E-W	2	0.35	0.13 – 0.53	0.47	0.26 – 0.67
		1	0.31	0.11 - 0.44	0.38	0.18 – 0.57
	N-S	2	0.43	0.13 – 0.60	0.46	0.30 – 0.60
		1	0.38	0.11 - 0.57	0.40	0.19 – 0.59
SC4-3	E-W	3	0.37	0.18 – 0.56	0.50	0.28 – 0.66
		2	0.28	0.13 – 0.37	0.32	0.15 – 0.49
		1	0.29	0.15 – 0.40	0.37	0.20 – 0.51
	N-S	3	0.41	0.19 – 0.53	0.51	0.30 – 0.65
		2	0.33	0.14 – 0.45	0.38	0.19 – 0.51
		1	0.33	0.15 – 0.43	0.39	0.24 – 0.53

Typical bidirectional response results from the second NLRHA series are presented in Figure 10 under a pair of orthogonal GM record components from a crustal EQ. In Figure 10a and 10b, peak storey drifts in level 1 occurred nearly simultaneously in both directions under this particular pair of GM records. In the E-W direction, larger storey drifts developed along Line 1 compared to those along Line 9. In the N-S direction, more consistent storey drifts developed along Lines A and F. In both directions, the structure returned to its original position, without residual deformations. This behaviour can also be seen from the E-W *vs* N-S first storey drift traces at the four building corners shown in Figures 10c and 10d.

Table 4 gives the statistics of peak first storey drifts along both the E-W and N-S directions obtained from the bidirectional response analysis. Drift values obtained along column lines that include the IV-BFs (lines 2 and 8 for E-W drifts and lines C and D for N-S drifts), as well at the four corners of the buildings are presented. As shown, when compared to the drifts obtained from unidirectional NLRHA, introducing 5% mass eccentricity in both directions and simultaneously applying orthogonal GM record components generally resulted in larger mean peak storey drifts at the IV-BFs as well as at the building corners. As expected, increases at the building corners are larger, varying from 1.01 to 1.31, as those are located farther from the center of rigidity of the buildings compared to the IV-BFs, which resulted in maximum values among the GM ensembles reaching excessive drifts that could result in inelastic beam responses. In Table 5, higher peak floor and roof accelerations were also obtained from the second NLRHA series compared to the unidirectional NLRHA series. These results clearly indicate that the proposed system can lead to torsion-sensitive buildings when responding nonlinearly to seismic GMs, even in case of symmetrical structures as those studied herein. One possible means of mitigating this effect is to increase the

torsional stiffness of the building by positioning the VB assemblies along the building perimeter. This option is examined is examined herein for the SC4-2 building by moving the VB assemblies on lines B and E to lines A and F, respectively, and those on lines 3 and 7 to lines 1 and 9, respectively, as shown in Figure 7b. In addition, the beam section of those VB assemblies was increased from W610x174 to W610x195. For this particular building, this modification had limited impact as mean peak drifts at the building corners reduced from 1.42% h_{s1} to 1.40% h_{s1} and from 0.97% h_{s1} to 0.96% h_{s1} in the E-W and N-S directions, respectively, and mean peak floor and roof accelerations remained practically unchanged. Other strategies such as positioning the stiffer IV-BFs on the exterior column lines should be examined in future studies.

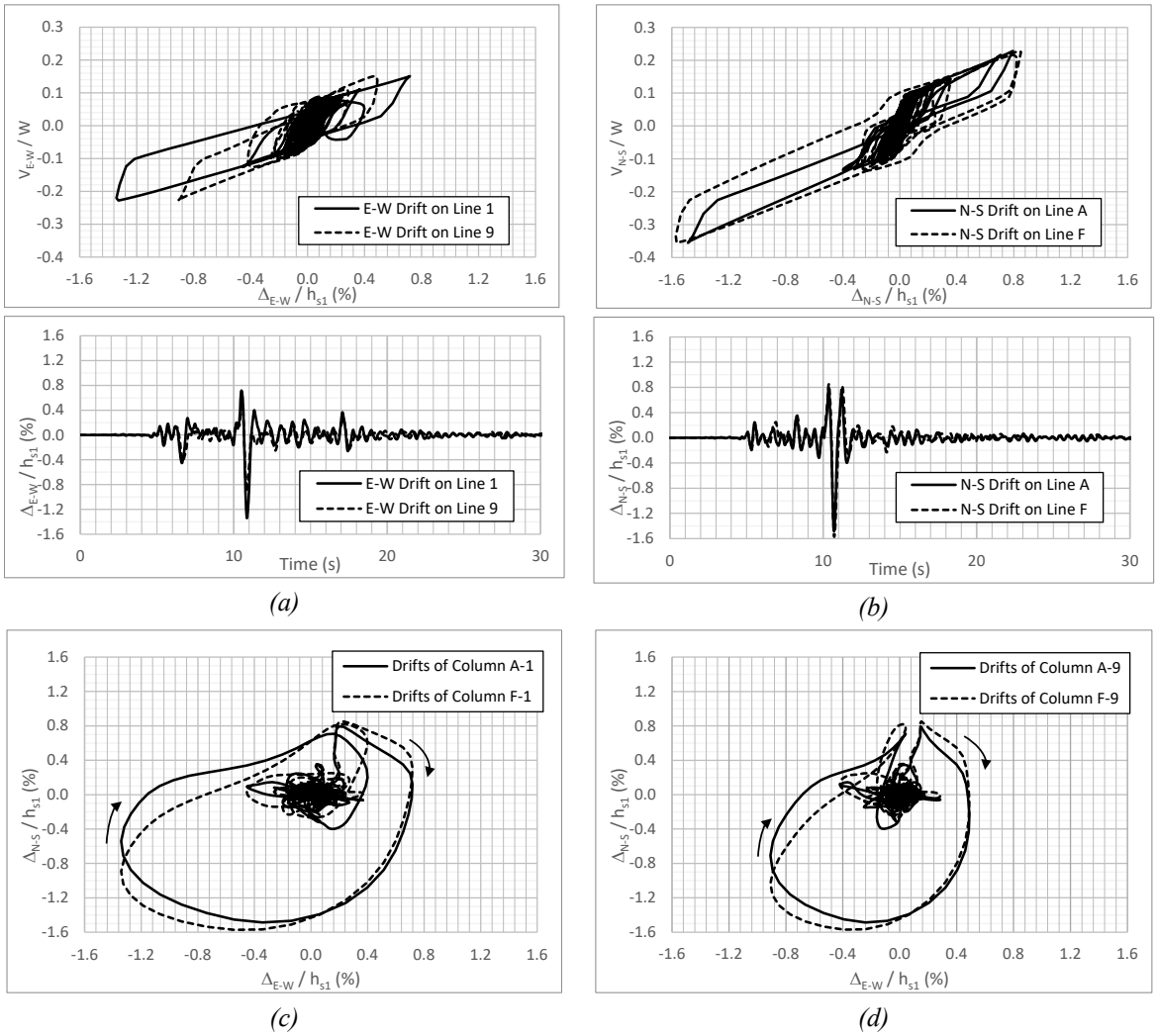

Figure 10. First-storey response of the SC4-3 structure under the 20° (N-S) and 110° (E-W) components of the 1994 M6.69 Northridge EQ, LA Saturn Street records: (a) E-W response; (b) N-S response; (c) N-S vs E-W storey drifts at building corners on Line 1; (d) N-S vs E-W storey drifts at building corners on Line 9.

CONCLUSIONS

This article introduced an innovative simple braced frame system specially designed and detailed to develop an elastic nonlinear self-centering storey shear *vs* storey drift response at the first level of low-rise steel building structures to cat as a base isolation system to achieve superior damage-free response in case of moderate and strong earthquakes. The proposed system was described together with the equations for determining the effective stiffness and equivalent damping properties of the system that can be used when applying the simple single-mode analysis method for the design of base isolated systems. To illustrate the design of the proposed system, validate its seismic behaviour and validate the applicability of the single-mode design approach for predicting lateral displacements, the proposed system was applied to 2- and 3- storey buildings located in Montreal, QC, for eastern Canada, and Vancouver, BC, for western Canada, and NLRHA was performed using ensembles of design level site-representative seismic ground motion to examine their response.

When subjected to unidirectional ground motions applied independently along each building principal direction, the proposed system was found to behave as intended, i.e., exhibiting lateral self-centering elastic response with lateral displacements concentrated in the first level and no residual deformations. Mean values of the peak first-storey drifts were close to those to those predicted with the single-mode analysis method. Peak floor and roof horizontal accelerations were less than the peak ground accelerations at the site, confirming that the system can act as a base isolation system to reduce seismic loads imposed to building structures during earthquakes.

Larger storey drifts and horizontal accelerations were obtained, however, when using three-dimensional building models with accidental mass eccentricity of 5% the building dimensions in both directions and simultaneously applying pairs of orthogonal ground motion components along both directions, which suggests that the system can become sensitive to in-plane torsional response when responding to earthquakes in the nonlinear range. This aspect will need to be investigated further in future studies to propose improvements to the system and/or the design method to reliably mitigate these effects.

ACKNOWLEDGMENTS

Funding for this project was provided by the Natural Sciences and Engineering Research Council (NSERC) of Canada.

REFERENCES

[1] Zhong, C., and Christopoulos, C. (2022). "Self-centering seismic-resistant structures: Historical overview and state-of-the-art," *Earthquake Spectra,* 38(2), 1321-1356.
[2] Kelly, J.M. (1990). "Base isolation linear theory and design," *Earthquake Spectra*, 6(2), 223-244.
[3] Kelly, J.M. (2005). "Seismic isolation of civil buildings in the USA," *Progress Struct. Eng. Maths*, 1(3), 279-285.
[4] Makris, N. (2019). "Base isolation: early history," *Earthquake Engng Struct Dyn.*, 48, 269-283.
[5] Martel, R.R. (1929). "The effects of earthquakes on buildings with a flexible first story," *Bull. Seismological Soc. of America*, 167-178.
[6] Green, N.B. (1935). "Flexible first-storey construction for earthquake resistance," *ASCE Transactions*, 100(1), 645-652.
[7] Fintel, M., and Khan, F.R. (1969). "Shock-absorbing soft story concept for multistory earthquake structures," *ACI Journal*, 381-390.
[8] Akiyama, H. (1985). *Earthquake-Resistant Limit-State Design for Buildings*, Univ. of Tokyo Press, Tokyo, Japan, 372 pp.
[9] Esteva, L. (1992). "Nonlinear seismic response of soft-first-story buildings subjected to narrow-band earthquakes," *Earthquake Spectra*, 8(3), 373-389.
[10] Uno, T., Yabe, Y., Ikura, K., Mase, S., Hirama, T., Shimizu, H., Kato, M., Ohtake, F., Terada, T., and Kanemitsu, T. (1993). *Earthquake resistant multi-story building*," US. Patent No. 5271197, The United States Patent and Trademark Office (USPTO).
[11] Hodogaya, T., and Akiyama, H. (1998). "Seismic design of flexible-stiff mixed frame with energy concentration," *Eng. Struct.*, 20(12), 1039-1044.
[12] Sutcu, F., Inoue, N., and Hori, N. (2006). "Energy based damper design of a structure with a displacement controlled soft-story," *Proc. 8th U.S. Nat. Conf. on Earthquake Eng.*, San Francisco, CA, Paper no. 260.
[13] Palermo, M. Ricci, I., Gagliardi, S., Silvestri, S. Trombetti, T., and Gasparini, G. "Multi-performance seismic design through an enhanced first-storey isolation system," *Eng. Struct.*, 59, 495-506.
[14] Benavent-Climent, A., and Mota-Páez, S. (2017). "Earthquake retrofitting of R/C frames with soft first story using hysteretic dampers: Energy-based design method and evaluation," *Eng. Struct.*, 137.
[15] Yazdi, H.A., Hashemi, M.J., Al-Mahaidi, R., and Gad, E. (2021). "Multi-axis testing of concrete-filled steel tube columns forming ductile soft-story in multi-story buildings," J. of Constr. Steel Res., vol. 183, 2021.
[16] Rakesh, E.N., Parvez, I.A., and Kumar, A. (2017). "Study on dynamic P-delta effects of a building with soft storey," *Int. J. of Eng. Res. In Mech and Civil Eng.*, vol. 2(4).
[17] Canadian Commission on Building and Fire Codes - CCBFC (2022). *National Building Code of Canada 2020*. Prepared by the CCBFC, National Research Council of Canada, Ottawa, ON.
[18] Canadian Standard Association – CSA (2019). *CAN/CSA-S16: Design of Steel Structures.* Prepared by the CSA, Toronto, ON.
[19] Natural Resources Canada - NRC (2021). *2020 NBC Seismic Hazard Tool.* Prepared by Natural Resources Canada, Ottawa, ON. 2020 National Building Code of Canada Seismic Hazard Tool (nrcan.gc.ca)
[20] McKenna, F., Scott, M.H., and Fenves, G. L. (2010). "Nonlinear finite element analysis software architecture using object composition." *J. Comput. Civ. Eng.*, 24(1), 95-107.
[21] Computers & Structures, Inc. (2023). SAP2000 Ultimate, v23.2.0, Computers & Structures, Inc., Walnut Creek, CA, USA. https://www.csiamerica.com